REPORT DOCUMENTATION PAGE

Form Approved
OMB No. 0704-0188

1. REPORT DATE *(DD-MM-YYYY)* 23-06-2013	**2. REPORT TYPE** Final Report	**3. DATES COVERED** *(From - To)* 04/01/2012 -03/31/2013

4. TITLE AND SUBTITLE
A Finite-Rate Gas-Surface Interaction Model Informed by Fundamental Computational Chemistry Simulations

5a. CONTRACT NUMBER
FA9550-12-1-0202

5b. GRANT NUMBER

5c. PROGRAM ELEMENT NUMBER

6. AUTHOR(S)
Schwartzentruber, Thomas, E.

5d. PROJECT NUMBER

5e. TASK NUMBER

5f. WORK UNIT NUMBER

7. PERFORMING ORGANIZATION NAME(S) AND ADDRESS(ES)
Regents of the University of Minnesota
Office of Sponsored Projects Admin
200 Oak St. SE
Minneapolis, MN 55455

8. PERFORMING ORGANIZATION REPORT NUMBER

9. SPONSORING / MONITORING AGENCY NAME(S) AND ADDRESS(ES)
AF Office of Scientific Research
875 N Randolph St., Rm 3112
Arlington, VA 22203

10. SPONSOR/MONITOR'S ACRONYM(S)

11. SPONSOR/MONITOR'S REPORT NUMBER(S)

12. DISTRIBUTION / AVAILABILITY STATEMENT
A - Approved for public release

13. SUPPLEMENTARY NOTES

14. ABSTRACT

A finite-rate gas-surface model (for use as a CFD boundary condition) specific to oxygen-silica reactions was formulated using computational chemistry calculations. A new interatomic potential was developed (and made publicly available) specifically for oxygen-silica gas-surface reactions (ReaxFF-SiO-GSI) using a large database of density functional theory single point energies. Computational chemistry calculations predicted a number of surface defects on realistic silica surfaces (in agreement with experimental data) which participate in the surface recombination of oxygen. The dominant reaction pathways occurring on these defects were studied by MD simulations of oxygen impacts. Steric factors and activation energies were computed for each reaction and the resulting model was formulated to satisfy detailed balance. The dominant mechanisms were found to not be activated processes (no energy barriers), resulting in little temperature dependence on recombination efficiencies. Product molecules resulting from a single collision-based reaction were found to not thermally accommodate to the surface, rather they leave in excited vibrational levels. The new finite-rate model and thermal accommodation results can be directly used in CFD calculations.

15. SUBJECT TERMS
High temperature gas-surface interactions Molecular Dynamics Computational Fluid Dynamics

16. SECURITY CLASSIFICATION OF:			**17. LIMITATION OF ABSTRACT**	**18. NUMBER OF PAGES**	**19a. NAME OF RESPONSIBLE PERSON**
					Thomas Schwartzentruber
a. REPORT	**b. ABSTRACT**	**c. THIS PAGE**	UU	17	**19b. TELEPHONE NUMBER** *(include area code)*
UU	UU	UU			612-625-6027

Standard Form 298 (Rev. 8-98)
Prescribed by ANSI Std. Z39.18

A Finite-Rate Gas-Surface Interaction Model Informed by Fundamental Computational Chemistry Simulations

Grant/Contract Number: FA9550-12-1-0202
Program Manager: Dr. John Schmisseur

PI: Thomas E. Schwartzentruber
Aerospace Engineering and Mechanics,
University of Minnesota
Phone: 612-625-6027 Fax: 612-626-1558 Email: schwartz@aem.umn.edu

1-Year Grant (April 1, 2012 through March 31, 2013)

DOCUMENT CONTENTS:

*NOTE: The research performed under the current grant is a (1-year) continuation of the work performed under completed AFOSR Grant: FA9550-09-0157. Thus sections I. and II. of the current report are identical to sections I. and II. of the final report for the prior grant (FA9550-09-0157), and are included as background material.

I. Introduction and Existing State-of-the-Art

Vehicles traveling through an atmosphere at hypersonic speeds generate strong shock waves. These shock waves generate extremely high gas temperatures within the shock layer between the shock itself and the surface of the vehicle. As the gas reaches such high temperatures, its vibrational degrees of freedom become excited and diatomic and polyatomic molecules dissociate into reactive atomic species. At high altitudes characteristic of hypersonic flight where the free-stream density is low, these reactive species diffuse through the boundary layer and may chemically react with the vehicle's thermal protection system (TPS). Many TPS materials act as a catalyst for the heterogeneous recombination of dissociated species back into molecules. Such exothermic surface reactions transfer additional energy to the vehicle surface and thus contribute to the heat flux and overall heat load that the TPS must withstand. For example, studies have shown that surface catalysis can contribute up to 30% of the total heat load for Earth reentry [1].

Typically at the beginning of the design phase of a TPS, 100% catalytic efficiency is assumed at the vehicle surface. This provides an upper-limit, conservative estimation for the heating rates. For 100% catalytic efficiency, all dissociated atoms impacting the surface are assumed to leave the surface as recombined molecules. Later in the design cycle the boundary conditions may be relaxed to a parameterized catalytic efficiency (using a recombination rate γ, that is a function of temperature and pressure) if such data exists for the specific gas and solid conditions involved. As outlined in a recent review article on the status of aerothermal modeling [2], such data is very limited and contains large uncertainties. While lower and upper bounds on heating rates are certainly useful, depending on the flight conditions and atmosphere, these predictions can differ significantly [3]. An example of experimental data obtained on RCG coated Space Shuttle tiles [4] is shown below in Fig. 1. Here the atom recombination coefficient γ (for both oxygen and nitrogen atoms) is curve-fit to various functions of temperature.

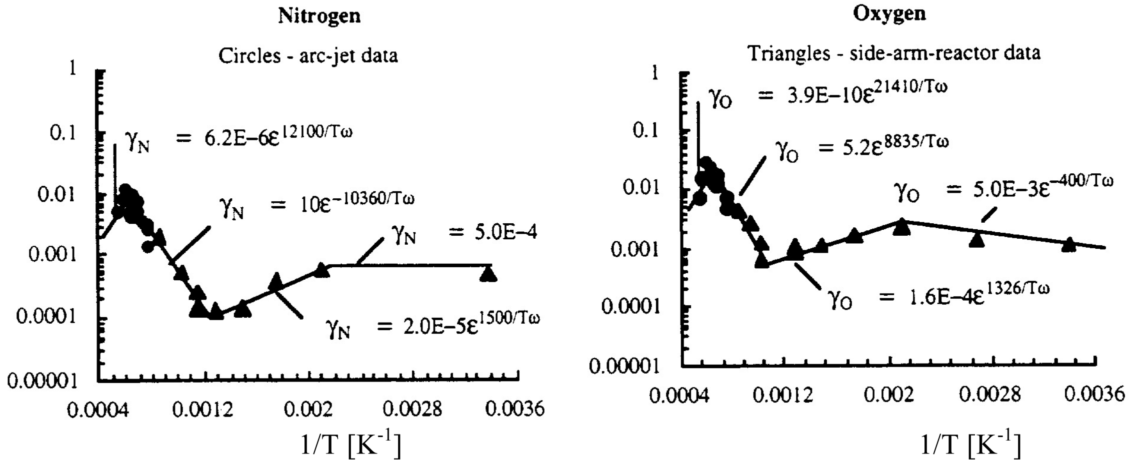

Figure 1 – Experimentally determined recombination rate (γ) as a function of temperature for RCG coated tiles (taken from [4] "Surface Catalysis and Characterization of Proposed Candidate TPS for Access-to-Space Vehicles", Stewart 1997).

Currently there is no fundamental explanation for these complex trends with temperature. It is possible the large changes in slope are due to different chemical mechanisms being "activated" at certain temperature thresholds, but these mechanisms are unknown. Inherently, the parameter γ represents the net effect of many elementary chemical mechanisms that collectively lead to recombination. As a result, it is difficult to relate variations in γ directly to fundamental surface chemistry. This inhibits a true understanding of the phenomenon and limits the transferability of the model. Furthermore, the high temperature data, obtained in arc-jet tests, are inferred from heat flux measurements. This requires an accurate model of the arc-jet flow field and predicted convective heat flux. When compared with the measured heat flux, the discrepancy is attributed to recombination, where full energy accommodation is also assumed. In fact, the arc-jet flow is poorly characterized and the assumption of full energy accommodation is not necessarily valid. Thus, extrapolation of these inferred γ values to flight conditions is not rigorous.

II. Prior Research Efforts

II.1 Finite-Rate Gas-Surface Models

A more fundamental model for gas-surface chemistry is analogous to the gas-phase finite-rate chemistry models that have been successfully used for many years. However, **in practice, the *parameterization* of such finite-rate gas-surface interaction models is extremely challenging** [1,5-14]**.** For gas-surface systems, the chemical reactions now involve gas-phase species as well as adsorbed species, and reactions should be made specific to various “chemical sites” on the surface. As an example, a test model for air is listed in Table 1. The model contains air species N_2, O_2, N, O, NO, as well as adsorbed atomic species denoted as A(s), metastable (diffusing) adsorbed species $A(s)_m$, and finally open surface sites [s]. The reaction mechanisms include adsorption/desorption reactions as well as Eley-Rideal (E-R) and Langmuir-Hinshelwood (L-H) recombination reactions. E-R reactions occur when a gas-phase atom strikes an adsorbed atom and recombines into a molecule that leaves the surface. L-H reactions occur when two adsorbed atoms diffuse into close proximity and recombine to form a molecule that leaves the surface. Reverse reactions of these processes are also included.

$\mathrm{O} + [\mathrm{s}] \underset{k_b^1}{\overset{k_f^1}{\rightleftharpoons}} \mathrm{O(s)}$	Adsorption/Desorption
$\mathrm{N} + [\mathrm{s}] \underset{k_b^2}{\overset{k_f^2}{\rightleftharpoons}} \mathrm{N(s)}$	Adsorption/Desorption
$\mathrm{O} + \mathrm{O(s)} \underset{k_b^3}{\overset{k_f^3}{\rightleftharpoons}} \mathrm{O_2} + [\mathrm{s}]$	E-R/Diss-Adsorption
$\mathrm{N} + \mathrm{N(s)} \underset{k_b^4}{\overset{k_f^4}{\rightleftharpoons}} \mathrm{N_2} + [\mathrm{s}]$	E-R/Diss-Adsorption
$\mathrm{O} + \mathrm{N(s)} \underset{k_b^5}{\overset{k_f^5}{\rightleftharpoons}} \mathrm{NO} + [\mathrm{s}]$	E-R/Diss-Adsorption
$\mathrm{N} + \mathrm{O(s)} \underset{k_b^6}{\overset{k_f^6}{\rightleftharpoons}} \mathrm{NO} + [\mathrm{s}]$	E-R/Diss-Adsorption
$\mathrm{O(s)}_m + \mathrm{O(s)} \underset{k_b^7}{\overset{k_f^7}{\rightleftharpoons}} \mathrm{O_2} + 2[\mathrm{s}]$	L-H/Diss-Adsorption
$\mathrm{N(s)}_m + \mathrm{N(s)} \underset{k_b^8}{\overset{k_f^8}{\rightleftharpoons}} \mathrm{N_2} + 2[\mathrm{s}]$	L-H/Diss-Adsorption
$\mathrm{O(s)}_m + \mathrm{N(s)} \underset{k_b^9}{\overset{k_f^9}{\rightleftharpoons}} \mathrm{NO} + 2[\mathrm{s}]$	L-H/Diss-Adsorption
$\mathrm{N(s)}_m + \mathrm{O(s)} \underset{k_b^{10}}{\overset{k_f^{10}}{\rightleftharpoons}} \mathrm{NO} + 2[\mathrm{s}]$	L-H/Diss-Adsorption

Table 1 – Gas-surface reactions for a generic air surface catalysis model.

The net flux mediated by the surface depends on the dynamics of each species on the active surface sites according to the mechanisms listed and on the rate constants associated with each mechanism. For example, the specific form of the E-R rate constant is shown in Table 2 with an initial qualitative parameterization [5]. Currently there is no way of experimentally determining all the required parameters and rate coefficients. However, these **parameters now have a direct physical link to fundamental chemistry**. Specifically, the coefficients correspond to activation energies (E), steric factors (γ), surface site concentrations (Φ_{total}), and kinetic flux quantities ($v/4$). In principle, the reaction mechanisms and parameters required for their rates could be determined by computational chemistry studies. Indeed, this approach has been successful for many *gas-*

Eley – Rideal

$\gamma_{er,O} = 0.001$

$\beta_O = 0$

$E_{er} = 9000\ J/mol$

$\Phi_{total} = 7.5 \times 10^{-6}\ mol/m^2$

$$k_f = \left(\frac{\bar{v}}{4\Phi_{total}}\right)\gamma_o T^{\beta} \exp\left(-\frac{E_{er}}{RT}\right)$$

Table 2 – Example of a test parameterization for the forward reaction rates.

phase finite-rate chemistry models currently in use and our research attempts to accomplish this for gas-surface finite-rate chemistry.

II.2 Computational Chemistry Studies of *Unphysical* Crystalline Surfaces

A substantial amount of previous research had been conducted in this area by two European research groups [15-16] and [17-21]. In fact, one group recently published an article (in 2011) where a finite-rate catalytic model is developed for air-silica interactions using computational chemistry simulations [21]. We have performed a thorough review of this prior work since it is so closely related to the main objectives of this AFOSR grant. Unfortunately, **during the early stages of our research for this grant, we quickly realized that these prior methodologies were completely inadequate for real materials used in hypersonic applications, and we found the conclusions of many of these studies to be invalid.** Since this AFOSR research report will present a new oxygen-silica finite rate catalytic model that is substantially different from this previously published work, a critical review of this prior work is warranted. A brief review follows that clearly **shows a large disconnect between the computational chemistry community and the aerothermodynamics community** for these problems and highlights some of the critical issues addressed by our AFOSR grant research.

Unphysical Bulk Material (Prior Studies):

Both research groups used computational chemistry techniques to investigate oxygen interactions with a specific crystalline polymorph of SiO_2 (called β-cristobalite). Computer images of this crystal lattice are shown in Fig. 2. The choice of β-cristobalite is motivated by experimental studies from Balat-Pichelin *et al.* [15,22,23] where silicon-carbide (SiC) surfaces were exposed to high temperature air-plasmas. During such exposure, an oxide layer was quickly formed and atomic oxygen loss-rates (recombination coefficients) were then determined next to the oxide layer surface. While the experimental measurements are of high quality and repeatability, the conclusion that the measured loss rates correspond to β-cristobalite was based on the fact that for polymorph diagrams of SiO2, β-cristobalite is most stable within the experimental surface temperature range. However, **it is almost impossible to imagine that a crystalline oxide layer was formed by exposing SiC to an air plasma**. Indeed, production of crystalline materials (such as quartz, another stable SiO_2 polymorph) requires careful and precise manufacturing techniques to slowly grow the crystal without introducing defects. Thus, **these prior studies are computationally investigating a different material than used in the experiments they compare with.** Rather, the oxide layer produced in the experiments is most likely amorphous SiO_2.

Unphysical Surface Structure (Prior Studies):

Furthermore, in order to simulate interactions with a *surface*, these prior studies simply "cleaved" the bulk crystal along the (001) plane (as seen in Fig. 2a) and then proceeded to study gas-phase collisions with this surface. However, such cleaved surfaces have highly unphysical dangling bonds (see the top layer of Si atoms in Fig. 2a). For example, these studies conclude (and we have confirmed) that any gas-phase oxygen that hits these dangling bonds will immediately adsorb (as seen in Fig 2b) with such a strong bonding energy that no future catalytic reaction could possibly remove this atom from the surface to form a molecule.

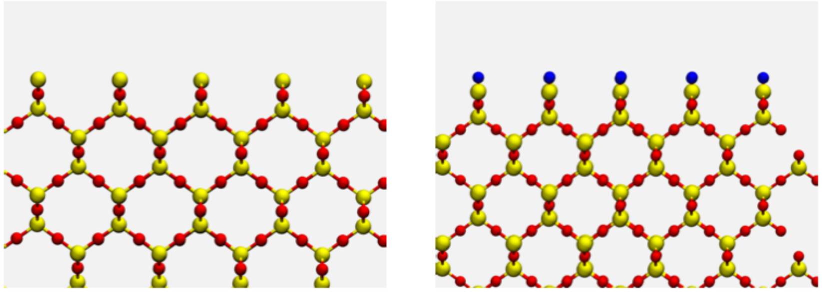

(a) Silicon Terminated (001) β-Cristobalite Surface (side)

(b) Oxygen Terminated (001) β-Cristobalite Surface (side). Topmost layer of oxygen highlighted in blue.

Figure 2 – Cleaved (001) β-cristobalite surfaces used in prior computational chemistry studies of surface catalysis under conditions relevant to hypersonic flight (Si – yellow, O – red, O originating from the gas are blue).

In order to study recombination, these previous studies instead placed adsorbed oxygen atoms at different (and less energetically bound) locations and then studied collisions with incoming gas-phase oxygen atoms. This now led to a certain rate of recombination reactions, which of course depended upon where the adsorbed oxygen was placed. By following this invalid modeling approach, remarkable agreement with measurements from air plasma experiments was reported [15,16]. In contrast, our computational chemistry simulations predict that such cleaved surfaces reconstruct into the lower-energy, stable surface configurations seen in Fig. 3. Such surface reconstructions are supported by a number of experimental studies that will be detailed later in this report. Thus, **not only is the bulk material (β-cristobalite) unphysical but, perhaps more importantly, the *surfaces* that gas-phase atoms interact with in these previous studies are not only physically unrealistic, but they are computationally unstable.**

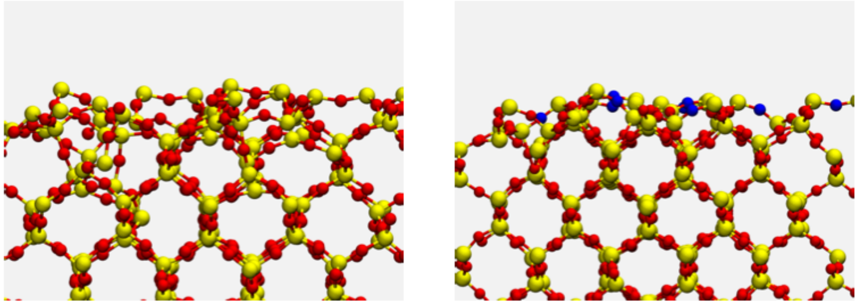

(a) Silicon Terminated (001) β-Cristobalite Surface (side)

(b) Oxygen Terminated (001) β-Cristobalite Surface (side). Topmost layer of oxygen are highlighted in blue.

Figure 3 – Surface reconstructions of (001) β-cristobalite (Si – yellow, O – red, O originating from the gas are blue).

Arbitrary Surface Coverage (Prior Studies):

Once probabilities of adsorption, desorption, and recombination are determined in function of surface temperature and gas-phase impact energy, one can develop a reaction rate model parameterized in function of the gas-surface temperature (T). If these rate equations are solved for a given partially-dissociated gas state (species concentrations, temperature, and pressure), the resulting concentrations of adsorbed species [A(s)] can be calculated from the reactions in Table 1. These adsorbed concentrations then correspond to a specific surface coverage corresponding to these specific gas conditions. **Determination of the surface coverage is extremely important, as it dictates the actual surface that gas-phase molecules interact with**. In the previously published finite rate model [21], the model predicted a steady-state coverage saturated with O_2 molecules for which no further recombination is possible. However, a surface coverage part-way between zero coverage and steady state was selected and recombination efficiencies for this arbitrary coverage were reported, which also happened to match experimentally determined values very well. There is no basis for assuming such an arbitrary surface coverage. In fact, a steady state surface coverage is established over very small time scales while catalytic reactions continue on the surface for macroscopic time scales. Thus, **the surface coverage assumed in prior studies was not representative of the experiments they compared with, and was even in contradiction with the computational chemistry simulations of the same studies.**

Improper Application of Detailed Balance and Unphysical Backwards Rates (Prior Studies):

Finally, as will be shown from our research, when forming a finite-rate chemistry model, **detailed balance must properly be accounted for such that reverse reaction rates and equilibrium states remain physically realistic**. Specifically, in the previously published rate model [21], the reverse rate of E-R recombination (dissociative adsorption of a gas-phase molecule) is very high and roughly equal to that of atomic oxygen adsorption. However, the O_2 surface impact simulations presented in the same publication do not find any dissociative adsorption reactions despite finding an atomic adsorption probability close to one. Furthermore, the reported desorption rate coefficient is higher than the theoretical limit (set by the vibrational frequency of O_2 molecules) by two orders of magnitude. Thus, this **previously published finite-rate catalytic model for oxygen-silica interactions contains backwards rates that are both unphysical and in contradiction with the computational chemistry simulations themselves.**

These prior studies [15-21] have been published in high quality computational chemistry and surface science journals. The above critical review clearly demonstrates the lack of rigorous collaboration and understanding between computational chemistry researchers and aerothermodynamics researchers. Specifically, the conclusions of our research under this AFOSR grant are that each of the above aspects, bulk material, surface structure, surface coverage, and detailed balance are crucial to developing a physically realistic and consistent finite rate model for oxygen-silica catalytic reactions.

II.3 Computational Chemistry Studies of Amorphous SiO_2 Surfaces

Dr. Cozmuta, published an AIAA conference paper in 2007 entitled, "Molecular mechanisms of gas surface interactions in hypersonic flow" [24]. In this paper, Cozmuta presented preliminary results for computational chemistry simulations of dissociated air interacting with an *amorphous* SiO_2 surface. The simulations began with a vacant amorphous SiO_2 surface exposed to partially-dissociated high temperature air. Recombination reactions were monitored only after the surface coverage reached a steady state. An image of such a simulation is shown in Fig. 4. This type of simulation is much more physically realistic than those performed in the studies reviewed above, and **Cozmuta's work provided the original framework for our AFOSR grant research**. Specifically, Cozmuta chose to use a reactive force-field to model inter-atomic forces, called ReaxFF. The unique ReaxFF formulation enables large scale Molecular Dynamics (MD) simulation while accurately modeling chemical reactions. ReaxFF will be described in detail in an upcoming section of this report.

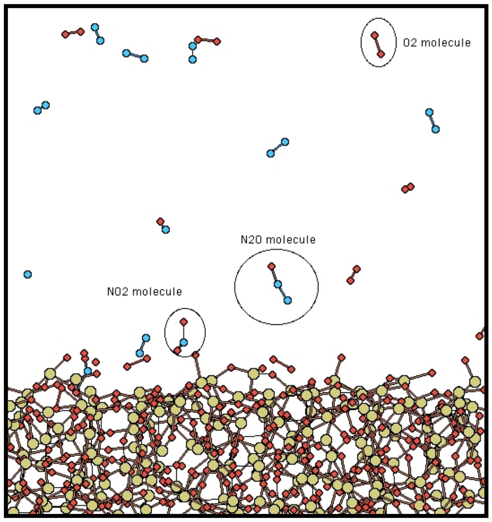

Figure 4 – ReaxFF MD simulations of dissociated air interacting with amorphous SiO_2.

III.1 A Finite-Rate Catalytic Model for Oxygen-Silica from Computational Chemistry

In this work we focus on surface catalysis of atomic oxygen on silica (SiO_2). **Silica is chosen because it is a significant component in both reusable** (LI900, LI2200, FRSI) **and ablative** (SIRCA) **thermal protection systems** [24]. In addition, studies have found that several non-SiO_2 based thermal protection systems, such as SiC (at T < 1800 K) and Ultra High Temperature Ceramics (ZrB2-SiC and ZrB2-SiC-HfB2 at T < 1300 K) form thin SiO_2 layers when exposed to air plasma, and act similarly to pure silica from a catalytic perspective [22,33]. Despite a large body of experimental work there is uncertainty in the precise temperature, pressure, and gas composition dependence of heating on silica surfaces due to heterogeneous catalysis [23]. **Reported values for oxygen recombination coefficients on silica** in the literature **span several orders of magnitude** ($2\text{x}10^{-4} < \gamma < 4\text{x}10^{-1}$) at 1000 K [34-35].

Our prior research (performed under AFOSR Grant FA9550-09-0157) detailed a complete methodology for formulating a finite rate gas-surface reaction model for oxygen-silica, through Molecular Dynamics simulations. Specifically, **this prior research used the $\text{ReaxFF}_{\text{SiO}}$ interatomic potential [28]**. Overall, this interatomic potential was quite accurate in that it successfully predicted a number of catalytic surface defects that have been observed experimentally [42,43]. However, the defect involved in the dominant recombination reaction pathway was a new prediction that had not been observed experimentally. Since the $\text{ReaxFF}_{\text{SiO}}$ potential was originally constructed for bulk silica and silica oxides, and not for gas-surface reactions, it was crucial that we verified these predictions before finalizing the rate model and moving on to other gas-phase species (such as nitrogen). Through an existing collaborative AFOSR MURI grant, which funded Prof. Don Truhlar's research group at the University of Minnesota, we had the opportunity to drastically increase the accuracy of our simulations. **For the current grant, we developed a new $\text{ReaxFF}_{\text{SiO}}^{\text{GSI}}$ potential, specifically constructed for oxygen-silica gas-surface interactions (GSI) [44]. This report describes the construction of the new $\text{ReaxFF}_{\text{SiO}}^{\text{GSI}}$ potential, makes concrete conclusions about the reactions occurring on realistic silica surfaces exposed to dissociated oxygen, and details a finalized finite-rate gas-surface reaction model for oxygen-silica systems that can be directly used in large CFD simulations.**

A New Interatomic Potential Developed Specifically for Oxygen-Silica Gas-Surface Interactions

The original $\text{ReaxFF}_{\text{SiO}}$ potential accurately predicted the bulk structure of amorphous-SiO_2 (a-SiO_2) and α-quartz, as well as a number of surface defect chemistries that participate in catalytic recombination reactions (example simulation images are depicted in Fig. 5 below). Since $\text{ReaxFF}_{\text{SiO}}$ was not developed for such defects and gas-surface reactions, we obtained a large number Density Functional Theory (DFT) energy calculations spanning a large number of configurations for each defect. Examples of these configurations are shown in Figs. 6(a) through 6(f) below.

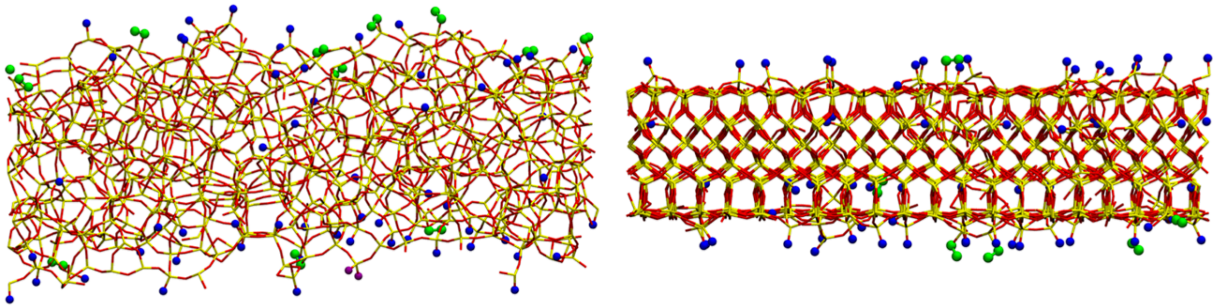

(a) a-SiO_2 slab

(b) Reconstructed (0001) α-quartz slab

Figure 5: Defects highlighted on silica surfaces after exposure to atomic oxygen. Defects are colored as NBO I (blue), NBO II (purple), peroxyl (green).

Essentially, all of the surface features predicted by the original ReaxFF$_{SiO}$ potential and interactions with atomic and molecular oxygen were analyzed in detail using DFT. As gas-phase atoms/molecules were moved relative to the defect sites, single point energies were extracted as seen in Figs. 7, 8, and 9. These energy curves were compared to the predictions of the original ReaxFF$_{SiO}$ potential, and were then used to fit the new ReaxFF$_{SiO}^{GSI}$ potential; greatly improving the accuracy.

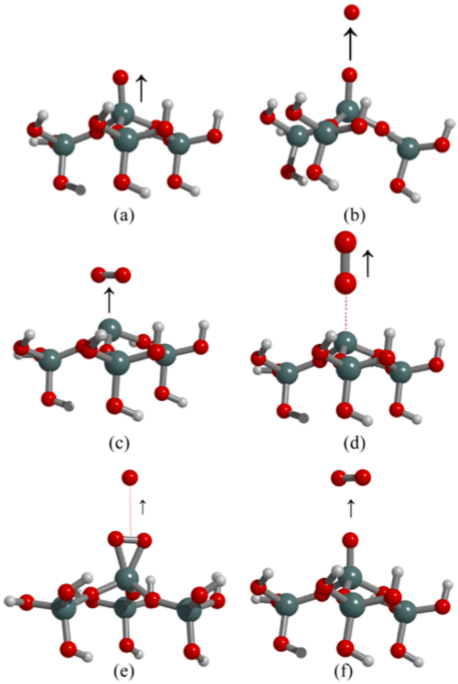

Figure 6: T4 Defect Clusters: (a) T4-O (b) T4-O+O (c) T4-O$_2$|| (d) T4-O$_2$_|_ (e) T4-O$_2$||+O (f) T4-O+O$_2$||

Whereas DFT predicts energies for both doublet (D) and quartet (Q) spin states, ReaxFF is always fit to the lowest energy spin-state. Figure 7 corresponds to the defect in Fig. 6(a) (an adsorbed oxygen). In this case, ReaxFF$_{SiO}$ is already in good agreement with DFT and predicts a strong binding energy of 5eV. Figure 8 corresponds to the configuration in Fig. 6(b) where an additional oxygen atom impacts the adsorbed oxygen. Here, there is an energy minimum corresponding to an adsorbed O$_2$ molecule, however, an energy barrier exists along this pathway. ReaxFF$_{SiO}$ did not predict the energy minimum or the energy barrier accurately, whereas, the newly developed ReaxFF$_{SiO}^{GSI}$ accurately captures both. Finally, Fig. 9 corresponds to Fig. 6(d) where the adsorbed oxygen molecule is seen to have a moderate energy barrier to overcome in order to leave the surface. In this case, the ReaxFF$_{SiO}$ potential is inaccurate, however, even the new ReaxFF$_{SiO}^{GSI}$ potential is incapable of a precise fit to the DFT data. This is because ReaxFF is fit to the lowest energy DFT result, and is not able to model spin-coupling. **Thus, the new ReaxFF$_{SiO}^{GSI}$ potential is much more accurate than the original ReaxFF$_{SiO}$ potential, however, the predicted binding energies and energy barriers have accuracy limitations due to the complexity of the energy surface.**

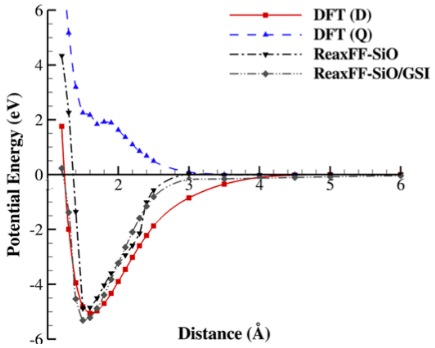

Figure 7: Energy curves for the T4-O cluster

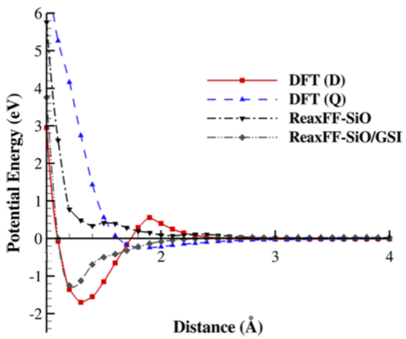

Figure 8: Energy curves for the T4-O+O cluster

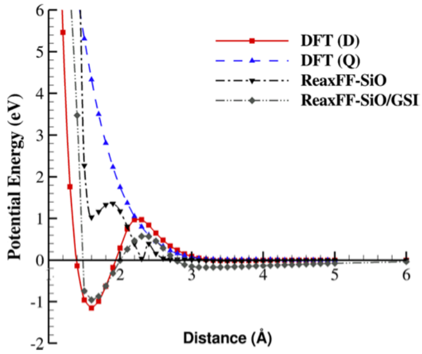

Figure 9: Energy curves for the T4-O$_2$_|_ cluster

The Dominant Catalytic Defect Chemistry (The Peroxyl Defect)

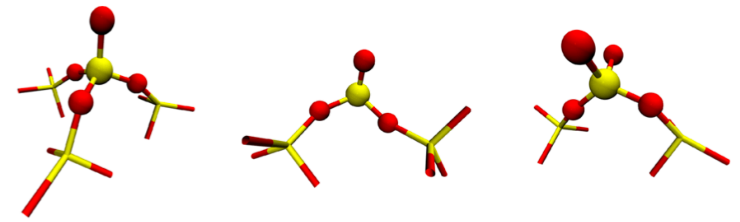

(a) Non-bridging oxygen defect I (NBO I)

(b) Non-bridging oxygen defect II (NBO II)

(c) Non-bridging oxygen defect III (NBO III)

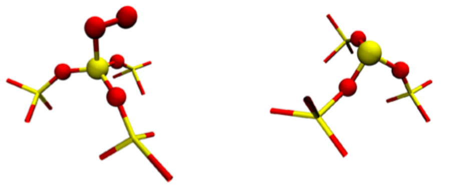

(d) Peroxyl defect

(e) Undercoordinated silicon defect (Si-UC)

Figure 10: Surface defects. Oxygen atoms (red) and silicon atoms (yellow).

The new $\mathrm{ReaxFF}_{\mathrm{SiO}}{}^{\mathrm{GSI}}$ potential predicts the same defect structures (all shown in Fig. 10) as the original $\mathrm{ReaxFF}_{\mathrm{SiO}}$ potential. However, when using the new (more accurate) $\mathrm{ReaxFF}_{\mathrm{SiO}}{}^{\mathrm{GSI}}$ potential, the geometry of the dominant defect (adsorbed molecular oxygen) is slightly altered into a peroxyl defect (Fig. 10d). The peroxyl defect has, in-fact, been observed experimentally [45], which lends much confidence to the newly constructed $\mathrm{ReaxFF}_{\mathrm{SiO}}{}^{\mathrm{GSI}}$ potential. To further verify this structure predicted by the new $\mathrm{ReaxFF}_{\mathrm{SiO}}{}^{\mathrm{GSI}}$ potential, we performed further DFT calculations of this defect and found that it is indeed an energetically favorable (stable) defect that would be expected to participate in recombination reactions. The $\mathrm{ReaxFF}_{\mathrm{SiO}}{}^{\mathrm{GSI}}$ predictions are compared to DFT in Table 3 below, where it is seen to successfully predict the geometry of this defect structure, although the binding energy is under-predicted by 1eV (a fairly substantial margin that will be discussed later). Thus all of the defects predicted by $\mathrm{ReaxFF}_{\mathrm{SiO}}{}^{\mathrm{GSI}}$ MD simulations are rigorously verified by DFT calculations and supported by experimental evidence. **We therefore conclude that these are the actual defects (Figs. 10a through 10e) present on real amorphous silica surfaces exposed to dissociated oxygen at high temperature.** This is a crucial milestone, which now enables detailed investigation of reactions pathways that involve these defects, using both MD and DFT.

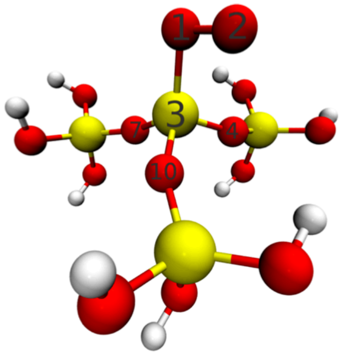

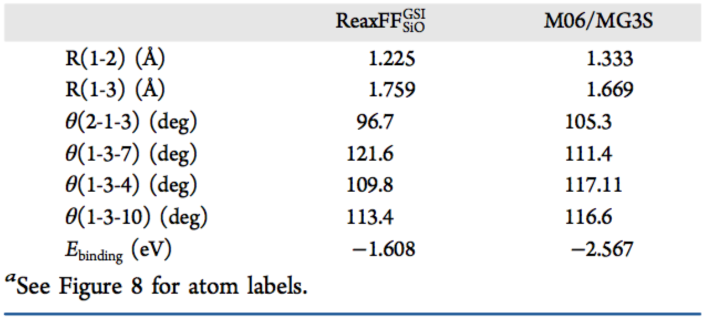

	$\mathrm{ReaxFF}^{\mathrm{GSI}}_{\mathrm{SiO}}$	M06/MG3S
R(1-2) (Å)	1.225	1.333
R(1-3) (Å)	1.759	1.669
θ(2-1-3) (deg)	96.7	105.3
θ(1-3-7) (deg)	121.6	111.4
θ(1-3-4) (deg)	109.8	117.11
θ(1-3-10) (deg)	113.4	116.6
E_{binding} (eV)	−1.608	−2.567

[a]See Figure 8 for atom labels.

Table 3: Geometric parameters and binding energy for the T4-O_2 cluster (with schematic of the cluster)

The Dominant Reaction Pathway Leading to the Surface Recombination of Oxygen

There is experimental evidence for the existence of the $(\equiv \mathrm{Si}\cdot)$ and $(\equiv \mathrm{Si}\text{-}\mathrm{O}\cdot)$ defects on silica surfaces under irradiation and fracture. The $(\equiv \mathrm{Si}\cdot)$ defect has been extensively studied, and has been identified on irradiated and vacuum fractured quartz and amorphous silica using Electron Spin Resonance (ESR) [46,47]. ESR in conjunction with isotope effects have been used to identify the $(\equiv \mathrm{Si}\text{-}\mathrm{O}\cdot)$ defect on irradiated amorphous SiO_2. The $(\equiv \mathrm{Si}\cdot)$ and $(\equiv \mathrm{Si}\text{-}\mathrm{O}\cdot)$ structures have also been observed in other MD simulations of a-SiO_2 surfaces simulated using different interatomic potentials [36,48,49]. The $(\equiv \mathrm{Si}\text{-}\mathrm{O}\cdot)$ defect is shown in Fig. 11a. Trajectories of oxygen atom impacts with this defect are shown in Fig. 11b, for which a high probability is found for the formation of an O_2 molecule on the surface in a peroxyl configuration. Thus, the $\mathrm{ReaxFF}_{\mathrm{SiO}}^{\mathrm{GSI}}$ MD simulations predict a significant amount of peroxyl defects. When subsequent oxygen atoms impact a peroxyl defect, this leads to an O_2 molecule leaving the surface into the gas phase. This can occur in two ways, either the adsorbed O_2 is completely replaced by the incoming oxygen atom (“O_2 replacement”), or the incoming atom bonds to the terminal oxygen on the peroxyl defect and the resulting molecule leaves the surface (called “ER Recombination II”). This is shown in Fig. 12a along with a potential energy scan of the interaction in Fig. 12b. It is evident that there is no energy barrier associated with either process, a conclusion that is fully supported by transition state DFT calculations. The probabilities of reaction pathways associated with the peroxyl defect and their dependence on the gas-surface temperature is shown in Fig. 13. As observed from Fig. 13, the dominant reaction pathway involves the release of O_2 (into the gas-phase) from a peroxyl defect with no associated energy barrier. As a result, recombination readily occurs on this defect and is not an activated process, leading to no temperature dependence in the reaction probability. This interesting result has ramifications for the behavior of the overall rate model that will be discussed in the next section.

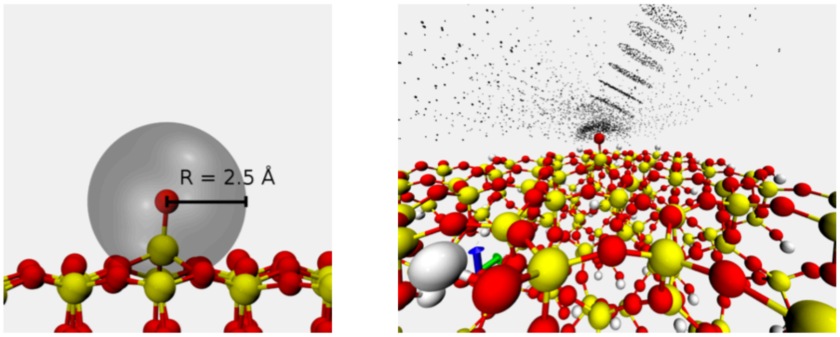

(a) Sites are considered as spheres having a radius of 2.5 Å, represented by the grey sphere

(b) Off normal collisions at $\phi = 30^o$ for the O + O_s reaction. Positions of impinging atoms shown every 250 time steps in black. Cluster is frozen in its minimum energy configuration

Figure 11: Trajectory calculations for oxygen atom impacts for the T4-O+O defect configuration.

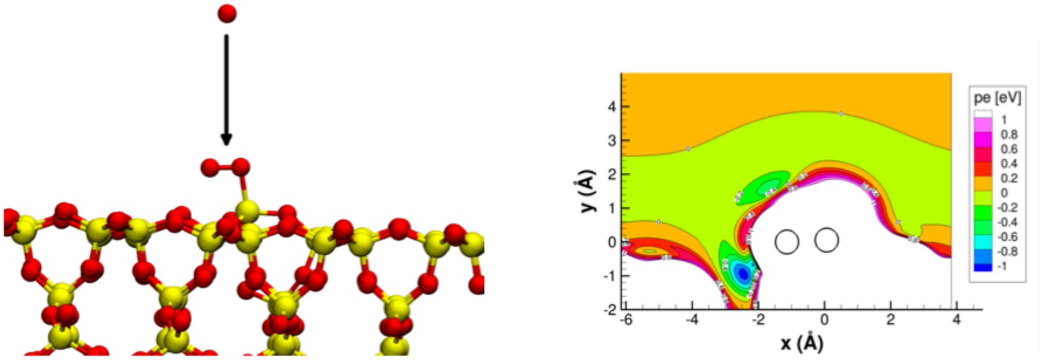

(a) Diagram of reaction

(b) Potential Energy Surface. Black circles represent location of oxygen atoms in the peroxyl defect

Figure 12: Potential energy surface for oxygen atom impacts on the peroxyl defect.

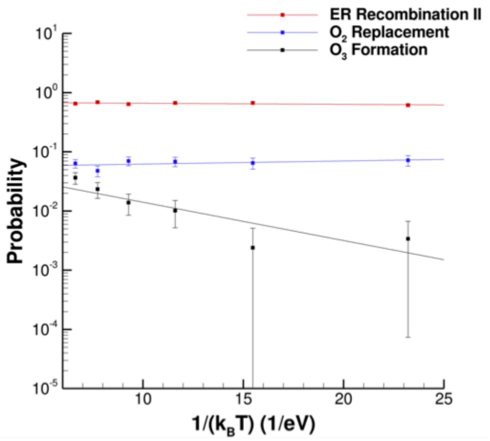

Figure 13: Reaction probabilities determined by large numbers of trajectory calculations on the peroxyl defect.

A Complete Finite-Rate Catalytic Model Predicted by the new $ReaxFF_{SiO}^{GSI}$ *Potential*

The finalized rate model is completely detailed below. The model formulation is identical to that constructed using the original $ReaxFF_{SiO}$ potential appearing in the final report of AFOSR Grant: FA9550-09-0157. However, the precise reactions, pre-exponential factors, and activation energies are now set based on the new results from the $ReaxFF_{SiO}^{GSI}$ potential and direct use of DFT data. We are currently preparing a journal article that details this model and all model parameters, so that other researchers can use this as a CFD boundary condition. All reactions, rate equations, and parameters are listed below. A detailed description of how this type of model can be incorporated into a CFD code is completely outlined in one of our recent journal papers [26].

Variable	Name	Units
$[O]$	Gas phase atomic oxygen concentration	$1/m^3$
$[O_2]$	Gas phase molecular oxygen concentration	$1/m^3$
$[O_s]$	Surface atomic oxygen concentration	$1/m^2$
$[O_{2s}]$	Surface molecular oxygen concentration	$1/m^2$
$[E_s]$	Surface empty site concentration	$1/m^2$
$[S]$	Total surface site concentration	$1/m^2$
θ_x	Surface coverage. (e.g. $\theta_o = [O_s]/[S]$)	
A_{site}	Area of a surface site	m^2

Reaction	Reaction Name	#
$O + E_s \rightleftharpoons O_s$	Atomic Oxygen Adsorption	1
$O + O_s \rightleftharpoons E_s + O_2$	ER Recombination	2
$O + O_s \rightleftharpoons O_{2s}$	O_2 Formation	3
$O + O_{2s} \rightleftharpoons O_s + O_2$	ER Recombination II/O_2 Replacement	4
$O_2 + E_s \rightleftharpoons O_{2s}$	Molecular Oxygen Adsorption	5

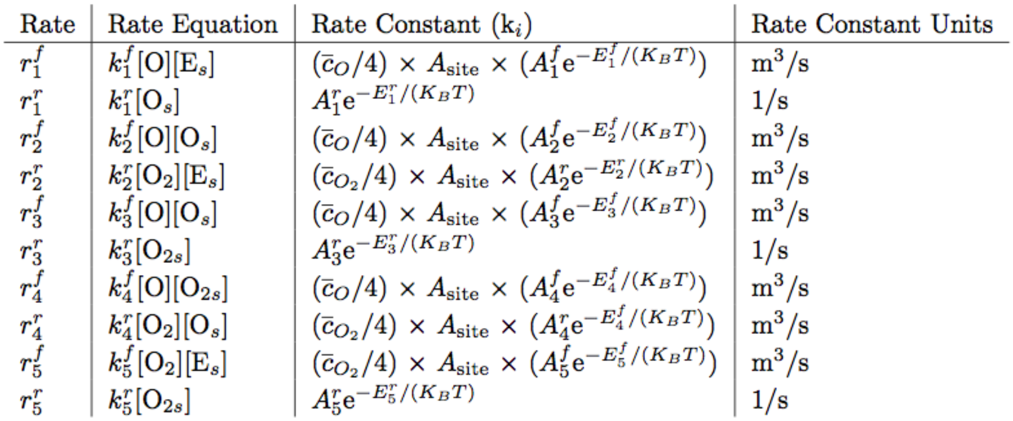

Rate	Rate Equation	Rate Constant (k_i)	Rate Constant Units
r_1^f	$k_1^f[\mathrm{O}][\mathrm{E}_s]$	$(\bar{c}_O/4) \times A_{\mathrm{site}} \times (A_1^f \mathrm{e}^{-E_1^f/(K_B T)})$	m^3/s
r_1^r	$k_1^r[\mathrm{O}_s]$	$A_1^r \mathrm{e}^{-E_1^r/(K_B T)}$	$1/\mathrm{s}$
r_2^f	$k_2^f[\mathrm{O}][\mathrm{O}_s]$	$(\bar{c}_O/4) \times A_{\mathrm{site}} \times (A_2^f \mathrm{e}^{-E_2^f/(K_B T)})$	m^3/s
r_2^r	$k_2^r[\mathrm{O}_2][\mathrm{E}_s]$	$(\bar{c}_{O_2}/4) \times A_{\mathrm{site}} \times (A_2^r \mathrm{e}^{-E_2^r/(K_B T)})$	m^3/s
r_3^f	$k_3^f[\mathrm{O}][\mathrm{O}_s]$	$(\bar{c}_O/4) \times A_{\mathrm{site}} \times (A_3^f \mathrm{e}^{-E_3^f/(K_B T)})$	m^3/s
r_3^r	$k_3^r[\mathrm{O}_{2s}]$	$A_3^r \mathrm{e}^{-E_3^r/(K_B T)}$	$1/\mathrm{s}$
r_4^f	$k_4^f[\mathrm{O}][\mathrm{O}_{2s}]$	$(\bar{c}_O/4) \times A_{\mathrm{site}} \times (A_4^f \mathrm{e}^{-E_4^f/(K_B T)})$	m^3/s
r_4^r	$k_4^r[\mathrm{O}_2][\mathrm{O}_s]$	$(\bar{c}_{O_2}/4) \times A_{\mathrm{site}} \times (A_4^r \mathrm{e}^{-E_4^f/(K_B T)})$	m^3/s
r_5^f	$k_5^f[\mathrm{O}_2][\mathrm{E}_s]$	$(\bar{c}_{O_2}/4) \times A_{\mathrm{site}} \times (A_5^f \mathrm{e}^{-E_5^f/(K_B T)})$	m^3/s
r_5^r	$k_5^r[\mathrm{O}_{2s}]$	$A_5^r \mathrm{e}^{-E_5^r/(K_B T)}$	$1/\mathrm{s}$

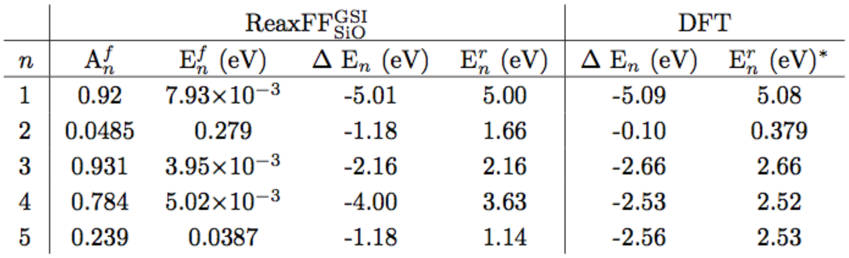

	$\mathrm{ReaxFF}_{\mathrm{SiO}}^{\mathrm{GSI}}$				DFT	
n	A_n^f	E_n^f (eV)	ΔE_n (eV)	E_n^r (eV)	ΔE_n (eV)	E_n^r (eV)*
1	0.92	7.93×10^{-3}	-5.01	5.00	-5.09	5.08
2	0.0485	0.279	-1.18	1.66	-0.10	0.379
3	0.931	3.95×10^{-3}	-2.16	2.16	-2.66	2.66
4	0.784	5.02×10^{-3}	-4.00	3.63	-2.53	2.52
5	0.239	0.0387	-1.18	1.14	-2.56	2.53

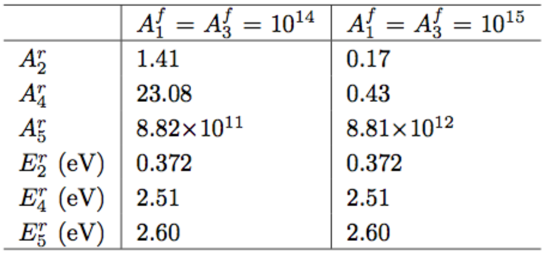

	$A_1^f = A_3^f = 10^{14}$	$A_1^f = A_3^f = 10^{15}$
A_2^r	1.41	0.17
A_4^r	23.08	0.43
A_5^r	8.82×10^{11}	8.81×10^{12}
E_2^r (eV)	0.372	0.372
E_4^r (eV)	2.51	2.51
E_5^r (eV)	2.60	2.60

This new model, supported by experimental evidence of the defect structures, and by a large database of DFT calculations results in a recombination coefficient (γ) that has a very weak temperature dependence. Thus, real silica surfaces contain defects that promote the catalytic recombination of oxygen with no significant energy barriers. Now that we have developed a fundamental understanding of precisely how oxygen recombines on silica surfaces, we can investigate how much of the chemical reaction energy is transmitted to the surface and how much remains in the internal energy modes of the recombined molecule (and is thus carried away from the surface). The degree of thermal accommodation of recombined species is a key input for CFD models, and is analyzed in the next section.

III.2 Vibrational Energy Accommodation

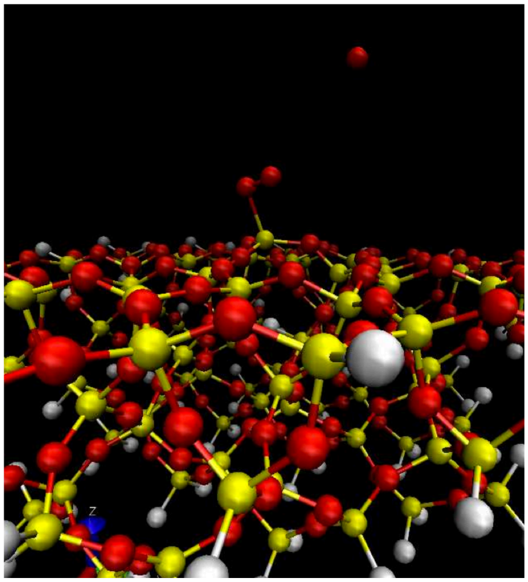

Figure 14: Snapshot of a trajectory simulation of vibrational energy accommodation resulting from a reaction on the peroxyl defect.

We ran a large number of trajectories on the peroxyl defect to study the vibrational energy of the recombined product molecules. A snapshot of such a trajectory calculation is shown in Fig. 14. The results are shown in Fig. 15. The translational, rotational, and vibrational energies of the recombined molecules were recorded for a large number of trajectories for a specific gas-surface temperature. This process was then repeated for a range of temperatures. The resulting energy budgets are shown in Fig. 15a, where it is evident that the molecules have vibrational energies well above the thermal energy of the surface. A large amount of energy is released during the recombination reaction on the peroxyl defect, and a significant amount of this energy stays in the vibrational mode of the product molecule, and therefore is not immediately transferred to the surface. The vibrational energy levels of recombined molecules are plotted in Fig. 15b. All of the gas-surface temperatures considered correspond to energies below the first vibrational level, however, the most probable energy levels of recombined molecules are between 5 and 10. This result is the first of its kind using an accurate potential ($\text{ReaxFF}_{\text{SiO}}^{\text{GSI}}$) and studying the peroxyl defect (the most dominant reaction pathway). Future studies could implement boundary conditions where the O2 molecules resulting from this reaction (ER-II – reaction #4) are given vibrational energies sampled from the distributions in Fig. 15b. It is interesting to note that such a boundary condition can not be readily implemented in a CFD code. This is due to the fact that through the use of a vibrational temperature (Tv), a CFD code is inherently assuming a Boltzmann vibrational energy distribution at all points in the flow, however, the boundary condition specified at the wall is very far from Boltzmann (Fig. 15b). Such a boundary condition is perfectly suited for direct simulation Monte Carlo (DSMC), however. In DSMC, simulated particles can be given any quantized vibrational energy level, and recombined molecules leaving a wall surface could be given energies directly sampled from the distributions in Fig. 15b. Of most interest would be the gas-phase energy transfer in the near wall region. These vibrationally excited molecules may transfer energy into rotational and translation modes of the gas through collisions, and this energy may be transferred back to the surface. Also vibrataionally excited molecules may be reflected back to the surface for multiple collisions and their vibrational energy may be "quenched" by the surface. Therefore, through multiple surface collisions and gas-phase energy transfer, the vibrational energy seen in Fig. 15b may, in-fact, be ultimately transferred to the surface (full accommodation). Thus, although on an individual gas-surface reaction basis, our results shown low thermal accommodation, when the full boundary layer is simulated this may lead to thermal accommodation. Such studies are certainly the next logical step.

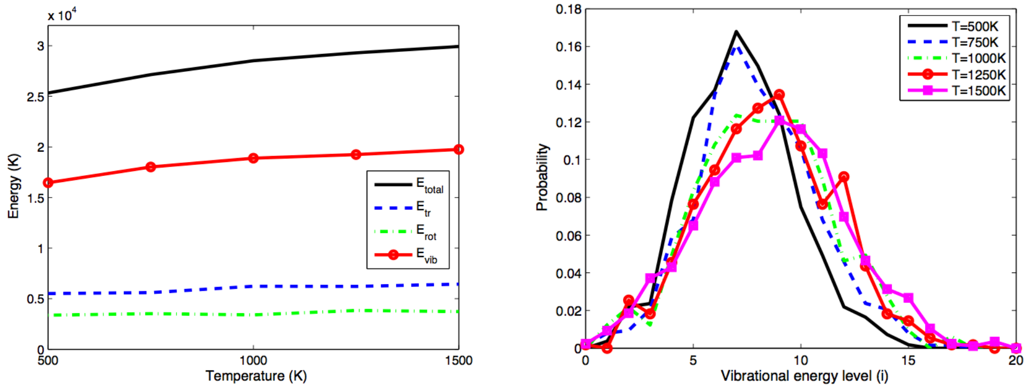

Figure 15: Energy budgets and vibrational energy distributions for recombined molecules.

III.3 Conclusions

The following conclusions are drawn from this research:

1) Catalytic recombination reactions on silica do not occur on the reconstructed crystal surfaces. Rather they occur on defects that occur naturally on amorphous silica surfaces but also on crystalline SiO_2 (such as quartz) when exposed to dissociated oxygen at high temperature.

2) The original $ReaxFF_{SiO}$ potential (developed for bulk silica polymorphs and oxides) successfully predicted the presence of many experimentally observed defects. Although Molecular Dynamics has its limitations (as discussed below), this predictive capability of $ReaxFF_{SiO}$ simulations was quite impressive. These $ReaxFF_{SiO}$ simulations of large realistic surfaces were crucial in order to direct more targeted computational chemistry (DFT) studies. However, for accurate quantitative predictions, we found that details matter, and the original $ReaxFF_{SiO}$ potential did not predict the precise geometry for what ultimately was the dominant defect leading to recombination reactions (the peroxyl defect). Also, the precision of the predictions for binding energies and energy barriers associated with these defects was limited and differed from DFT noticeably.

3) A new $ReaxFF_{SiO}^{GSI}$ potential was constructed using a large database of new DFT data. The resulting potential predicted the bulk structure of silica polymorphs as well as defects in agreement with experiment and DFT. The new $ReaxFF_{SiO}^{GSI}$ potential is completely described in Ref. [44] and the parameters are included (in LAMMPS format) as supplemental information; thus this new potential has been made freely available to all researchers in the field. With the defects identified and an accurate potential constructed, interactions between gas-phase oxygen atoms and molecules were studied with a large number of trajectories. Activation energies and pre-exponential factors were obtained from the trajectory analysis for reaction pathways associated with all defects.

5) After formulating the finite rate model, the dominant reaction pathway that most influenced the rate of recombination was an E-R type reaction on the peroxyl defect. This reaction was found by both MD and detailed DFT transition state analysis to be a non-activated process (no significant energy barrier). The ramification is that the overall finite rate model predicts almost no temperature dependence for the recombination efficiency (γ). This is in contrast to almost all prior models.

However, these prior models were not based on chemistry calculations or a physical understanding of specific chemical processes on real surfaces. Rather, these prior models were simply constructed to fit a weak temperature dependence found in a few (and widely variable) experiments. In fact, there are a number of alternate explanations for temperature dependence of recombination other than an activated ER process. For example, the experimental measurements were interpreted using simple diffusion models, which varied between experiments, and whose accuracy is questionable for high temperature dissociated air. Inaccuracy in the diffusion model could lead to an apparent temperature dependence of the interpreted recombination efficiency. As another example, the number of surface sites (defect sites) could be increasing with temperature, and this could be the cause of increased recombination at high temperatures (not an activated process). Finally, to generate atomic oxygen, the high temperature experiments required a plasma and so additional surface processes could be occurring in these experiments, beyond interactions with dissociated oxygen as studied in this work.

Therefore, our detailed computations predict non-activated recombination pathways are present on real silica surfaces (on defect sites supported by experimental evidence). Thus, any temperature dependence of the recombination efficiency should not be modeled as an activated ER reaction process, as our results conclude that these are non-activated reaction pathways.

6) The recombined molecules resulting from the dominant reaction pathway (ER recombination on the peroxyl defect) do not thermally accommodate to the surface. Molecules leave the surface in excited vibrational levels (levels 5-10) and thus not all of the chemical energy released by the reaction gets transferred to the surface ($\beta_{coll}<1$). However, when surface roughness and boundary layer processes are

included, the effective accommodation coefficient (β_{eff}) may approach one. This should be the focus of future work.

The current one-year grant is being directly continued under a new Basic Research Initiative (BRI) grant from the AFOSR (Grant # FA9550-12-1-0486). This new grant funds collaborative DFT, MD, and DSMC calculations with new experimental data to further this line of research.

IV. Publications Resulting from AFOSR Research Grant

Norman, P., Schwartzentruber, T.E., Leverentz, H., Luo, S., Meana-Paneda, R., Paukku, Y., and Truhlar, D.G., "The Structure of Silica Surfaces Exposed to Atomic Oxygen", J. Phys. Chem. C, 2013, 117, 9311-9321.

- This grant had a short 1-year period and work is now continuing under an AFOSR BRI grant
- The above publication is an important one where the atomistic structure of real defective silica surfaces is determined. This article, now serves as a crucial milestone for studying reactions with silica surfaces in detail.

V. REFERENCES:

[1] Barbato, M., Reggiani, S., Bruno, C., and Muylaert, J., "Model for Heterogeneous Catalysis on Metal Surfaces with Applications to Hypersonic Flows," Journal of Thermophysics and Heat Transfer, Vol. 14, No. 3, 2000, pp. 412–420.

[2] Wright, M.J., Olejniczak, J., Edquist, K.T., Venkatapathy, E., and Hollis, B.R., "Status of Aerothermal Modeling for Current and Future Mars Exploration Missions", IEEEAC paper #1428, Version 7, December 10, 2005.

[3] Bose, D., Wright, M. J., and Palmer, G. E., "Uncertainty Analysis of Laminar Aeroheating Predictions for Mars Entries," Journal of Thermophysics and Heat Transfer, Vol. 20, No. 4, October-December 2006, pp. 652–662.

[4] Stewart, D.A., "Surface Catalysis and Characterization of Proposed Candidate TPS for Access-to-Space Vehicles", NASA Technical Memorandum 112206, July 1997, Ames Research Center.

[5] J. Marschall and M. MacLean, "Finite-Rate Surface Chemistry Model, I: Formulation and Reaction System Examples", AIAA Paper 2011-3783, presented at the 42nd AIAA Thermophysics Conference, Honolulu, Hawaii, June 2011.

[6] Rosner, D. E. and Feng, H. H., "Energy Transfer Effects of Excited Molecule Production by Surface-catalyzed Atom Recombination," Faraday Trans.I - Phys.Chem., Vol. 70, 1974, pp. 884-907.

[7] Halpern, B. and Rosner, D. E., "Chemical energy accommodation at catalyst surfaces. Flow reactor studies of the assocation of nitrogen atoms on metals at high temperatures," J. Chem. Soc., Faraday Trans. 1, Vol. 74, 1978, pp. 1883–1912.

[8] Seward, W. A. and Jumper, E. J., "Model for Oxygen Recombination on Silicon-Dioxide Surfaces," Journal of Thermophysics and Heat Transfer, Vol. 5, No. 3, 1991, pp. 284–291.

[9] Deutschmann, O., Riedel, U., and Warnatz, J., "Modeling of Nitrogen and Oxygen Recombination on Partial Catalytic Surfaces," Journal of Heat Transfer, Vol. 117, 1995, pp. 495–501.

[10] Nasuti, F., Barbato, M., and Bruno, C., "Material-Dependent Catalytic Recombination Modeling for Hypersonic Flows," Journal of Thermophysics and Heat Transfer, Vol. 10, No. 1, 1996, pp.131-136.

[11] Armenise, I., Barbato, M., Capitelli, M., and Kustova, E.V., "State to State Catalytic Models, Kinetics and Transport in Hypersonic Boundary Layers," Journal of Thermophysics and Heat Transfer, Vol.20, No. 3, 2006, pp. 465-476.

[12] Thömel, J., Lukkien, J. J., and Chazot, O., "A Multiscale Approach for Building a Mechanism based Catalysis Model for High Enthalpy CO2 Flow," 39th AIAA Thermophysics Conference, Vol. AIAA 2007-4399, June 2007.

[13] Armenise, I., Capitelli, M., and Longo, S., "Fourier and Diffusive Heat Transfer in Hypersonic Nitrogen

Flows: State-to-State Approach," Journal of Thermophysics and Heat Transfer, Vol.23, No. 4, 2009, pp. 674-683.

[14] MacLean, M., Marschall, J., and Driver, D. M., "Finite-Rate Surface Chemistry Model, II: Coupling to Viscous Navier-Stokes Code," 42nd AIAA Thermophysics Conference, Honolulu, HI, Vol. AIAA Paper 2011-3784, June 2011.

[15] Bedra, L., Rutigliano, M., Pichelin, M. B., and Cacciatore, M., "Atomic Oxygen Recombination of Quartz at High Temperature: Experiments and Molecular Dynamics Simulation," Langmuir, Vol. 22, 2006, pp. 7208-7216.

[16] Cacciatore, M. and Rutigliano, M., "Eley-Rideal and Langmuir-Hinshelwood Recombination Coefficients for Oxygen on Silica Surfaces," Journal of Thermophysics and Heat Transfer, Vol. 13, No. 2, 1999.

[17] Arasa, C., Busnengo, H. F., Salin, A. and Sayos, R. [2008], 'Classical dynamics study of atomic oxygen sticking on the β-cristobalite (100) surface', Surface Science 602, 975–985.

[18] Arasa, C., Gamallo, P. and Sayos, R. [2005], 'Adsorption of atomic oxygen and nitrogen at β-cristobalite(100): A density functional theory study', Journal of Physical Chemistry B. 109, 14954–14964.

[19] Arasa, C., Moron, V., Busnengo, H. F. and Sayos, R. [2009], 'Eley-rideal reaction dynamics between o atoms on β-cristobalite(100) surface: A new interpolated potential energy surface and classical trajectory study', Surface Science 603, 2742–2751.

[20] Moron, V., Arasa, C. and Busnengo, H. F. [2008], 'Theoretical study of O2 dissociation and reflection on the β-cristobalite(100) surface', Proceedings of the Rarefied Gas Dynamics: 26th International Symposium, AIP Conf. Proc. 1084, 682.

[21] Moron, V., Gamallo, P., Martin-Gondre, L., Crespos, C., Larregaray, P. and Sayos, R. [2011], 'Recombination and chemical energy accommodation coefficients from chemical dynamics simulations: O/O2 mixtures reaction over a β-cristobalite (001) surface', Physical Chemistry Chemical Physics pp. 17494–17504.

[22] Balat-Pichelin, M., Badie, J., Berjoan, R. and Boubert, P. [2003], 'Recombination coefficient of atomic oxygen on ceramic materials under earth re-entry conditions by optical emission spectroscopy', Chemical Physics 291(2), 181–194.

[23] Bedra, L. and Balat-Pichelin, M. J. H., "Comparative modeling study and experimental results of atomic oxygen recombination on silica-based surfaces at high temperature," Aerospace Science and Technology, Vol. 9, 2005, pp. 318-328.

[24] Cozmuta, I., "Molecular mechanisms of gas surface interactions in hypersonic flow," 39th AIAA Thermophysics Conference, Miami, FL, 2007, AIAA-2007-4046.

[25] Nompelis, I., Drayna, T. W., and Candler, G. V., "A Parallel Unstructured Implicit Solver for Reacting Flow Simulation," 17th AIAA Computational Fluid Dynamics Conference, Vol. AIAA 2005-4867, June 2005.

[26] Sorensen, C., Valentini, P., and Schwartzentruber, T. E., "Uncertainty Analysis of Reaction Rates in a Finite Rate Surface-Catalysis Model," Journal of Thermophysics and Heat Transfer, Vol. 26, No. 3, 2012.

[27] Van Duin, A., Dasgupta, S., Lorant, F., and Goddard, W.A. III, "ReaxFF: A Reactive Force Field for Hydrocarbons", J. of Phys. Chem. A, 2001, I05, pp. 9396-9409.

[28] Van Duin, A., Strachan, A., Stewman, S., Zhang, Q., Xu, X., and Goddard, W.A. III, "ReaxFF$_{SiO}$ Reactive Force Field for Silicon and Silicon Oxide Systems", J. of Phys. Chem. A, 2003, I07, pp. 3803-3811.

[29] D. Frenkel and B. Smit. Understanding Molecular Dynamics Simulation. Academic Press, 2002.

[30] M. P. Allen and D. J. Tildesley. Computer Simulation of Liquids. Ox- ford, 1987.

[31] S. J. Plimpton. Fast parallel algorithms for short-range molecular dy- namics. J. Comp. Phys., 117:1–19, 1995.

[32] http://lammps.sandia.gov/index.html.

[33] Alfano, D., Scatteia, L., Monteverde, F., Beche, E., and Balat, M., “Microstructural characterization of ZrB2-SiC based UHTC tested in the MESOX plasma facility," Journal of the European Ceramic Society, Vol. 30, 2010, pp. 2345-2355.

[34] Kim, Y. C. and Boudart, M., “Recombination of O, N, and H Atoms on Silica:Kinetics and Mechanism," Langmuir, Vol. 7, 1991.

[35] Carleton, K. and Marinelli, W., “Spacecraft thermal energy accommodation from atomic recombination," Journal of Thermophysics Heat Transfer, Vol. 6, 1992, pp. 650-655.

[36] Levine, S. M. and Garofalini, S. H., “A structural analysis of the vitreous silica surface via a molecular dynamics computer simulation," The Journal of Chemical Physics, Vol. 86, No. 5, 1987, pp. 2997-3002.

[37] Chen, Y., Cao, C., and Cheng, H., “Finding stable alpha-quartz surface structures via simulations," Applied Physics Letters, Vol. 93, 2008, pp. 181911.

[38] Hu_, M., Demiralp, E., Cagin, T., and Goddard, W., “Factors a_ecting molecular dynamics simulated vitreos silica structures," Journal of Non-Crystalline solids, , No. 253, 1999, pp. 133-142.

[39] Jee, S., McGaughey, A., and Sholl, D., “Molecular simulations of hydrogen and methane permeation through pore mouth modified zeolite membranes," Molecular Simulation, Vol. 35, No. 1, 2010.

[40] Nakano, A., Kalia, R., and Vashishta, P., “First sharp diffraction peak and intermediate-range order in amorphous silica: finite-size defects in molecular dynamics simulations," Journal of Non-Crystalline Solids, Vol. 171, 1994, pp. 157-163.

[41] Susman, S., Voline, K., Montague, D., and Price, D., “Temperature dependence of the first sharp diffraction peak in vitreous silica," Physical Review B., Vol. 43, No. 13, 1991.

[42] Norman, Schwartzentruber, T.E., and Cozmuta, I., “A Computational Chemistry Methodology for Developing an Oxygen-Silica Finite Rate Catalytic Model for Hypersonic Flows”, AIAA Paper 2011-3644, June 2011, presented at the 42nd AIAA Thermophysics Conference, Honolulu, HI.

[43] Norman, P. and Schwartzentruber, T.E., “A Computational Chemistry Methodology for Developing an Oxygen-Silica Finite Rate Catalytic Model for Hypersonic Flows: Part II”, AIAA Paper 2012-3097, June 2012, presented at the 43rd AIAA Thermophysics Conference, New Orleans, LA.

[44] Kulkarni, A.D., Truhlar, D.G., Srinivasan, S.G., van Duin, A.C.T., Norman, P., and Schwartzentruber, T.E., “Oxygen Interactions with Silica Surfaces: Coupled Cluster and Density Functional Investigation and the Development of a New ReaxFF Potential”, *J. Phys. Chem. C*, 2013, 117, 258-269

[45] Griscom, D. L. Friebele, E. J., “Fundamental Defect Centers in Glass: Si Hyperfine Structure of the Nonbridging Oxygen Hole Center and the Peroxyl Radical in a-SiO2”, Phys. Rev. B, 1981, 24, 4896−4898.

[46] Warren, W., Poindexter, E., O_enberg, M., and Muller-Warmuth, W., “Paramagnetic Point Defects in Amorphous Silicon Dioxide and Amorphous Silicon Nitride thin Films," Joural of the Electrochemical Society, Vol. 139, No. 3, 1992.

[47] Costa, D., Fubini, B., Giamello, E., and Volante, M., “A novel type of active site at the surface of crystalline SiO2 (α-quartz) and its possible impact of pathogenicity," Canadian Journal of Chemistry, Vol. 69, 1991, pp. 1427-1434.

[48] Wilson, M. and Walsh, T., “Hydrolysis of the amorphous silica surface. I. Structure and dynamics of the dry surface." The Journal of Chemical Physics, Vol. 113, No. 20, 2000, pp. 9180-9190.

[49] Roder, A., Kob, W., and Binder, K., “Structure and dynamics of amorphous silica surfaces," Journal of Chemical Physics, Vol. 114, No. 17, 2001, pp. 7602-7614.